

Open system quantum annealing in mean field models with exponential degeneracy

Kostyantyn Kechedzhi¹ and Vadim N. Smelyanskiy²

¹*QuAIL, NASA Ames Research Center, Mail Stop 269-3, Moffett Field, CA 94035 and
USRA, NASA Ames Research Center, Moffett Field, CA 94035*

²*Google, 150 Main St, Venice Beach, CA, 90291*

Real life quantum computers are inevitably affected by intrinsic noise resulting in dissipative non-unitary dynamics realized by these devices. We consider an open system quantum annealing algorithm optimized for a realistic analog quantum device which takes advantage of noise-induced thermalization and relies on incoherent quantum tunneling at finite temperature. We analyze the performance of this algorithm considering a p -spin model which allows for a mean field quasiclassical solution and at the same time demonstrates the 1st order phase transition and exponential degeneracy of states. We demonstrate that finite temperature effects introduced by the noise are particularly important for the dynamics in presence of the exponential degeneracy of metastable states. We determine the optimal regime of the open system quantum annealing algorithm for this model and find that it can outperform simulated annealing in a range of parameters.

I. INTRODUCTION

Quantum computing hardware is affected by substantial level of intrinsic noise and therefore naturally realizes dissipative quantum dynamics^{1,2}. Optimization algorithms, where a configuration of a binary string x minimizing a given (energy or cost) function $f(x)$ is sought for, naturally extract computational advantage from the irreversible dissipative dynamics, and could therefore be readily implemented on a number of existing hardware platforms^{3,4}. More specifically, quantum annealing⁵ (QA) is a quantum analog of the widely applied classical simulated annealing algorithm⁶ (SA), a heuristic solver of NP-hard optimization problems^{5,7–10}, with quantum fluctuations playing the role analogous to thermal fluctuations in simulated annealing. NP-hard optimization problems such as finding a ground state spin configuration of a spin glass, are often characterized by an energy landscape with a large number of local minima separated by extensive energy barriers. Dissipative dynamics realized by the open system quantum annealing provides an efficient mechanism for thermalization within domains of attraction of local minima. For efficient search of the configuration space the barriers separating different domains of attraction have to be overcome which may proceed via thermal excitation or quantum tunneling process. The performance of the open system quantum annealing algorithm is therefore characterized by a set of relaxation rates associated with such processes, as opposed to, for example, the spectral gaps, as is the case for adiabatic quantum algorithm^{9,11}.

The longest relaxation times correspond to the often exponentially slow transitions between local minima separated by extensive potential barriers. Unitary dynamics of a pair of such states corresponds to the switching rate of the order of the matrix element Δ , which in presence of an extensive barrier may scale exponentially with the system size $\Delta \propto \exp(-\text{const} \times N)$. Whereas fast dissipative relaxation within a domain of attraction of a local minima due to the hardware noise introduces a lifetime

or level width W . This fast local relaxation strongly suppresses the coherent superposition of the states localized in different local minima when $W \gg \Delta$. Nevertheless, the incoherent quantum tunneling is possible in presence of such strong dissipation where the transition rate is described by the Fermi golden rule type expression $\propto \Delta^2 \ll \Delta$. This is the regime likely realized in a large scale quantum annealer³. It is an open question whether such incoherent extensive quantum tunneling may provide a more efficient mechanism for searching the configuration space as compared to classical simulated annealing relying on thermal excitation.

In this paper, we analyze the performance of the open system quantum annealing algorithm optimized for the regime of the quantum dissipative dynamics, taking advantage of thermalization and incoherent quantum tunneling. Our goal here is to analyze the contribution of extensive quantum tunneling to the performance of the algorithm. We consider a model in which there exists a metastable state separated by an extensive barrier from the ground state. We consider a system of Ising spins interacting each with each other with p -body interaction of equal strength, a model often referred to as a p -spin model. This model allows for a quasiclassical WKB description^{12,13}, where the expansion is performed in $1/N$ rather than the more usual \hbar , and, at the same time, demonstrates key features characteristic of a range of complex (NP-hard) optimization problems, such as the 1st order phase transition (for $p \geq 3$) and exponentially small gap between the ground and excited state. Crucially, the metastable state realized in this model is characterized by an exponential degeneracy whereas the ground state is unique. Such entropic imbalance is in fact typical for low energy states in the spin glass phase and it strongly affects the low temperature system dynamics in both quantum and classical cases. The effect of entropic imbalance is the main focus of our analysis in this paper.

We demonstrate that in presence of such extensive entropy imbalance SA computation time scales exponentially with the system size N . This can be understood

intuitively considering the performance of the simulated annealing applied to a model demonstrating a 1st order phase transition into a state characterized by an order parameter. Assume the ordered state to be a ferromagnet for simplicity. In simulated annealing the system is initialized at infinite temperature, or equal occupation of all classical spin states, then the temperature is gradually lowered to zero. The simulated spin dynamics is chosen to satisfy the detailed balance condition such that it samples the thermal distribution at a given (instant) temperature. The initial state is a paramagnet, and therefore the solution, the ground state spin configuration at zero temperature, is expected to have high statistical weight only at low enough temperatures below the ferromagnetic phase transition. The exponential degeneracy of the metastable state corresponds to the entropy linear in the system size N which significantly lowers the transition temperature. This can be understood intuitively from the following argument. We assume a mean field case in which energies of the metastable and ground states as well as the barrier separating them scale linearly with the system size NE_{MS} , NE_{GS} and NU , respectively. We find from equating the free energies $NQ_{MS} - NE_{MS}/T \approx -NE_{GS}/T$, where the entropy imbalance is given by NQ_{MS} , that the transition occurs at $T_c \sim \frac{E_{MS}-E_{GS}}{Q_{MS}} \sim O(1)$. Furthermore, high statistical weight of the ground state is achieved only after equilibration at the low temperature below the phase transition $T \lesssim T_c \sim O(1)$. In presence of the extensive barrier NU the relaxation towards the thermal distribution described by the classical Kramers escape rate $\sim \exp(-NU/T_c)$ is exponentially slow. Moreover, the entropy gradient along the over-the-barrier escape trajectory gives rise to an additional entropic factor $\sim \exp(Q_{MS} - Q_T)$, where Q_T is the entropy corresponding to the top of the barrier, which appears as an exponential contribution to the prefactor of the Kramers rate¹⁴. Therefore the computation time allowing for such relaxation to occur is at least as long the relaxation time $\tau_u \sim \exp(NUQ_{MS}/(E_{MS} - E_{GS}) + Q_{MS} - Q_T)$. In fact, a more careful analysis, see Appendix A, shows that the optimal SA computation time in the presence of the extensive entropy imbalance is given by the smallest of either τ_u or the exhaustive search time $\tau_{es} \sim 2^N$. At the same time quantum tunneling amplitude saturates as $T \rightarrow 0$ and may be more efficient than over the barrier escape suggesting that quantum annealing could be more efficient than simulated annealing. Note however that quantum tunneling rate in this mean field model will also scale exponentially with N . Therefore the performance of each algorithm will be characterized by a numerical factor in the exponent which have to be carefully compared. The result is not obvious a priori since we are comparing here different microscopic mechanisms: the quantum dynamics constrained by conservation laws with the classical thermal excitation process constrained by the entropy imbalance and the low temperature.

Considering the open system quantum annealing ap-

plied to the p -spin model we show that the scaling of the optimal QA computation time (allowing for repeated runs of the algorithm) is determined by the quantum tunneling amplitude at a single point in the algorithm, the so called freezing point, after which quantum/thermal fluctuations are weak and the transitions over or through the barrier are no longer likely. We find that due to the effect of the entropy associated with the metastable state the optimal quantum tunneling rate is achieved at vanishing temperature, i.e. raising temperature may reduce the quantum tunneling rate. This is in contrast with the usual intuition about a quantum mechanical particle trapped in a non-degenerate metastable potential well where the escape rate monotonously increases with temperature. The optimal QA regime therefore also corresponds to the vanishing temperature. Comparing the optimal computation time of QA obtained in this regime with that of SA for a range of the potential barrier shapes we find that QA could outperform SA under certain circumstances, thus providing a polynomial (rather than exponential) speedup.

The remainder of the paper is organized as follows. In Sec. II we introduce the p -spin model and its WKB analysis describing the evolution of the potential energy and the transition rates in the course of the quantum annealing algorithm. In Sec. III we discuss the dynamics of the model in the course of the quantum annealing and identify the freezing point and its optimal position in the course of the algorithm. We conclude with a discussion of the results in Sec. IV.

II. THE MODEL

We consider N Ising spins $1/2$ on a fully connected graph (i.e. each spin interacts with each other spin) with uniform interaction strength such that the system is fully described in terms of the total spin projection operator $\hat{S}^\alpha = \sum_{i=1}^N \hat{\sigma}_i^\alpha$, where $\alpha = x, y, z$ and $\hat{\sigma}^\alpha$ is a set of spin- $1/2$ operators. We consider a Hamiltonian,

$$\mathcal{H} = sNf\left(\frac{2}{N}\hat{S}^z\right) - (1-s)\hat{S}^x, \quad (1)$$

consisting of a uniform transverse field term, the second term above, and a potential energy of interaction $f(x)$, which is assumed to be a function of the z -projection operator. The potential energy of a p -spin interaction of unit strength $H = \left(\frac{2}{N}\right)^p \sum \hat{\sigma}_{i_1}^z \hat{\sigma}_{i_2}^z \dots \hat{\sigma}_{i_p}^z$ corresponds to $f(x) = x^p$. Without loss of generality we choose both of the terms in the Hamiltonian Eq. (1) to scale linearly with N . The parameter s in Eq. (1) controls the relative strength of the potential energy and the transverse field and changes from $s = 0$ to $s = 1$ in the course of the quantum annealing algorithm.

Of specific interest is the case of $p = 3$. Models with $p > 3$ can be solved in polynomial time by avoiding the

1st order phase transition using advanced driver Hamiltonian, b -spin ($b \geq 2$) interactions inducing transverse (XY) ferro- or antiferromagnetism, in addition to the standard transverse field term^{15–17}. In this case arriving at the ground state at the end of the QA evolution does not require extensive quantum tunneling through a barrier. Therefore a classical model algorithm such as “spin-vector” Monte Carlo method¹⁸, which could follow the deformation of the effective quasiclassical potential imitating the course of QA, is also not expected to encounter a bottleneck requiring exponential computation time. Whereas in the case of $p = 3$ the 1st order phase transition cannot be avoided in this way, as a result an exponentially weak tunneling process is critical for finding the ground state in this system. The quantum tunneling regime in this case cannot be described by a classical model. While adiabatic quantum computation was analyzed in the p -spin model^{19,20}, we will focus here on the open system quantum annealing in presence of dissipation and non-zero temperature which is the case more suitable for implementation on current analog quantum annealers.

The Hamiltonian Eq. (1) commutes with $\hat{S}^2 \equiv (\hat{S}^x)^2 + (\hat{S}^y)^2 + (\hat{S}^z)^2$, which is therefore a conserved quantity. In the basis of states, $|S, M\rangle : \hat{S}^2|S, M\rangle = S(S+1)|S, M\rangle$, with definite total spin S and its projection on z -axis $M = \{-S, \dots, S\}$ the matrix elements of the Hamiltonian Eq. (1) are given by the standard spin- S rules,

$$\hat{S}^z|S, M\rangle = M|S, M\rangle \quad (2)$$

$$\hat{S}^\pm|S, M\rangle = \sqrt{S(S+1) - M(M \pm 1)}|S, M \pm 1\rangle \quad (3)$$

where we introduced raising and lowering operators, $\hat{S}^\pm = \frac{1}{2}(\hat{S}^x \pm i\hat{S}^y)$. We introduce an integer parameter $K = 0, 1, \dots, \lfloor \frac{N}{2} \rfloor$ to label the total spin eigenstates $S = \frac{N}{2} - K$, each value corresponding to a completely disconnected subspace of the eigenspace of Eq. (1), which will however be connected due to the coupling to a thermal bath. The Hamiltonian Eq. (1) is symmetric with respect to exchanges of pairs of spins $\hat{\sigma}_i \leftrightarrow \hat{\sigma}_j$, and in fact with respect to all permutations of spins, since such operations do not change the sum over all spins \hat{S}^α . This symmetry introduces a high degeneracy of eigenstates depending on their total spin S . The subspace with the maximal total spin $S = \frac{N}{2}$ or $K = 0$ contains $2S + 1$ non-degenerate states (there are no non-trivial permutations) corresponding to all possible projections of the total spin on z -axis. At the same time the states with $K \neq 0$ are highly degenerate, with the degeneracy being determined by the representations of the group of permutations. The eigenstate with a total spin labeled by K has the degeneracy $\binom{N}{K} - \binom{N}{K-1} \sim \exp(NQ_k)$, where $k \equiv \frac{K}{N} = \{0, \frac{1}{N}, \frac{2}{N}, \dots, \frac{1}{N} \lfloor \frac{N}{2} \rfloor\}$, which corresponds to the entropy term,

$$Q_k \approx -k \ln k - (1-k) \ln(1-k) + O\left(\frac{\ln N}{N}\right),$$

that has to be added to the free energy of a state with a given energy E and total spin parameter k , $\mathcal{F} = \beta E + Q_k$.

In this paper we are interested in a cubic potential energy,

$$f(q) = -c(q - q_{min})^2 \left(q - \frac{3q_{max} - q_{min}}{2} \right), \quad (4)$$

where $q \equiv \frac{2}{N}M$, $q = \{-(1-2k), \dots, (1-2k)\}$. Eq. (4) is the most general cubic function with the metastable minimum at q_{min} and the potential barrier top at q_{max} , where $f(q_{min}) > f(1)$ ensures that $q = 1$ is the global minimum. Without loss of generality we can put $c = 1$, the only effect of $c \neq 1$ is to rescale the parameter s in Eq. (1).

The dynamics of the total spin can be described using a systematic quasiclassical WKB expansion¹². In a spin model this expansion is performed in terms of the small parameter $\varepsilon \equiv 2/N \ll 1$ which is an analog of \hbar in the textbook WKB approach²¹. We consider a wave function in the form,

$$\Psi = e^{i\frac{1}{\varepsilon}\Phi(q)},$$

and expand it, $\Phi(q) \approx \Phi_0 + \varepsilon\Phi_1 + \varepsilon^2\Phi_2 + O(\varepsilon^2)$. We can further expand the coefficients Φ_i for a small shift of the argument from q to $q \pm \varepsilon$,

$$\Psi_{M \pm 1} = \Psi_M e^{\pm i\dot{\Phi}_0} \left(1 + i\varepsilon_2 \ddot{\Phi}_0 \pm i\varepsilon \dot{\Phi}_1 \right)$$

where $\dot{O} \equiv \frac{dO}{dq}$. Substituting this expansion into the Schroedinger equation we obtain,

$$\mathcal{H}\Psi(q) \approx e(q)\Psi(q),$$

where in the main order in ε the Hamiltonian is diagonal and reads,

$$e(q) \approx sf(q) - \frac{1}{2}(1-s)\sqrt{(1-2k)^2 - q^2} \cos \dot{\Phi}_0. \quad (5)$$

Note that the function $p \equiv \dot{\Phi}_0$ is precisely the canonical momentum conjugate of the coordinate q , $p \rightarrow -i\frac{d}{dq}$. In other words the second term above is a quantum kinetic energy which for $p \ll 1$ corresponds to a particle with a position dependent mass $m^{-1} \equiv \frac{1}{2}(1-s)\sqrt{(1-2k)^2 - q^2}$ moving in an effective classical potential,

$$U(k, q) = sf(q) - \frac{1}{2}(1-s)\sqrt{(1-2k)^2 - q^2}. \quad (6)$$

Note that the mass of the effective quantum particle is position dependent, it increases with increasing q and diverges as $q \rightarrow 1$ which affects the efficiency of quantum

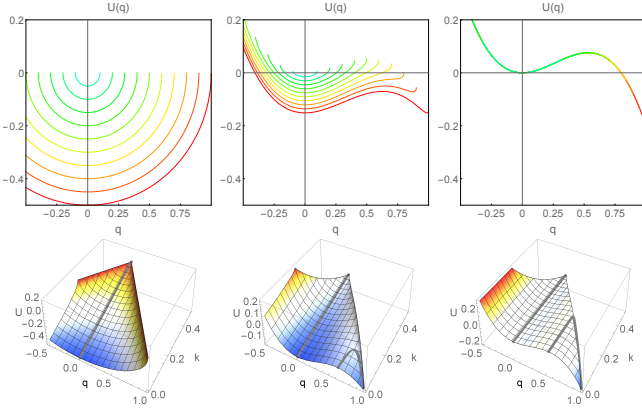


Figure 1. Effective classical potential is shown for $s = 0$, pure transverse field case (left), $s = s_{QPT} \approx 0.698$, the zero temperature quantum phase transition point (center), and $s = 1$, pure classical potential (right). Different lines (bottom to top on all plots) correspond to different values of $k = 0, \dots, 0.5$ with equal intervals. Note that in the absence of the transverse field the states with different values of k are degenerate. Here $q_{min} = 0$ and $q_{max} \approx 0.467$.

tunneling into the states near $q = 1$. The effective potential Eq. (6) for different values of s is shown in Fig. 1. In the course of the QA algorithm $s = 0 \rightarrow s = 1$ the effective potential deforms from a squareroot parabola corresponding to the ground state $(q, k) = (0, 0)$ with the maximal spin polarization along the transverse field direction at $s \rightarrow 0$, see left panel in Fig 1, and the classical potential corresponding to the ground state $(q, k) = (1, 0)$ fully polarized along the axis of quantization $s \rightarrow 1$. Note the initial and final states of the algorithm are characterized by exponentially small overlap, see Appendix B.

States with small kinetic energy are confined to one of the potential wells, centered around the two minima $q_{min}^{(L)}(s) < q_{min}^{(R)}(s)$ of the effective potential $U(k, q)$, which in the course of the evolution as $s \rightarrow 1$ approach the metastable $q_{min}^{(L)} \rightarrow q_{min}$ and ground state $q_{min}^{(R)} \rightarrow 1$ of the classical model, respectively. Confinement of the states is determined by the condition of vanishing classical velocity, $v(k, q, E) \equiv \frac{\partial \mathcal{H}}{\partial p} = 0$, which gives,

$$-1 \leq 2 \frac{sf(q) - E}{(1-s)\sqrt{(1-2k)^2 - q^2}} \leq 1. \quad (7)$$

The solution of this equation gives the location of the turning points $q_{TP}^{(1)}(k, E)$ and $q_{TP}^{(2)}(k, E)$ which limit the classically allowed region. Inverting the secular equation, Eq. (5) for a given energy E we write the wave function in the main order in ε ,

$$\Psi \sim \exp \left(\frac{i}{\varepsilon} \int_{q_{TP}^{(1)}}^q dp \right), \quad (8)$$

with

$$p = \arccos 2 \frac{sf(q) - E}{(1-s)\sqrt{(1-2k)^2 - q^2}}, \quad (9)$$

when the condition Eq. (7) is satisfied, and

$$p = i \operatorname{arccosh} 2 \frac{sf(q) - E}{(1-s)\sqrt{(1-2k)^2 - q^2}}, \quad (10)$$

otherwise. The latter expression corresponds to the exponentially decaying tail of the wave function extending beyond the classically allowed region into the potential barrier.

In the course of the evolution, $s : 0 \rightarrow 1$, there is a point of zero temperature discontinuous quantum phase transition, $s = s_{QPT}$, at which the minimal energies in the two wells, left E_L at $q \sim q_{min}$ and right E_R at $q \sim 1$, are equal to each other. In the course of the QA algorithm at finite temperature this transition occurs at a different transverse field strength $s = s_{PT}(\beta) \geq s_{QPT}$. The phase transition point can be found from the condition of equal occupation of the two potential wells $\mathcal{P}_L = \mathcal{P}_R$ including the entropy of the states. In the large N limit and at low temperatures $\beta \sim O(N^0)$ we can approximate the occupation number $\mathcal{P}_L = \sum_{E,k} \exp(-\mathcal{F} - \log Z) \approx \exp(-\mathcal{F}_L - \log Z)$ by a single dominant term corresponding to a minimum of the free energy. We write the local minimum condition in a potential well as $\frac{\partial \mathcal{F}}{\partial k} = 0$ to obtain,

$$-\beta \frac{\partial E}{\partial k} = -\frac{\partial Q_k}{\partial k} \approx \ln \frac{k}{1-k}. \quad (11)$$

This determines the k_{min} corresponding to the minimum of the free energy. Whereas the optimal energy (principal quantum number) with a given k corresponds to the minimum of the potential $U(k_{min}, q)$. We neglect the quantization of levels due to finite N for the purpose of this calculation. At $s > s_{PT}(\beta)$ the left potential well is separated from the ground state by a potential barrier with the shape determined by the parameters q_{min} and q_{max} and overall scaling $\sim N$. At low temperatures the relaxation in this model is therefore determined by the rate of transitions between the wells.

In a closed quantum system in the absence of the thermal bath multiple tunneling effects between the wells need to be taken into account which corresponds to the ground state formed by a coherent superposition of the states in the two potential wells, i.e. a Schrodinger cat state. In a large system the level splitting Δ corresponding to such superposition is exponentially small (in the system size N), and therefore such coherent dynamics is quickly suppressed by small perturbations, such as the hardware noise. This results in overdamped dynamics characterized by fast intra-well relaxation towards thermal occupation²² reflected in the level width $W \gg \Delta$ and exponentially rare incoherent tunneling effects with

the rate $\sim \Delta^2$. On the other hand we neglect the effect of noise on the tunneling event itself since tunneling is a fast process occurring on the timescale $1/\omega$, where ω is the frequency determined by the curvature of the potential. We assume therefore that $\omega \gg W \gg \Delta$. We are interested only in the exponential scaling of the transition rates in this paper ignoring the renormalization of the preexponential factor that may be substantial in the regime of strong coupling to the environment. Note that the overdamped dynamics and thermalization are expected even in the absence of the coupling to a thermal bath, it can be introduced by a weak disorder in the spin-spin interactions $\delta H = \sum \varepsilon_{ij} \hat{\sigma}_i^z \hat{\sigma}_j^z$ or even weak random transverse field²³.

In the regime of the overdamped dynamics at $s < s_{PT}(\beta)$ the ground state corresponds to $q = q_{min}^{(L)}(s)$. As the system goes past the phase transition with growing $s > s_{PT}(\beta)$ this state becomes metastable. The average transition rate $w \ll W$ across the barrier in presence of fast the intra-well relaxation W can be obtained by calculating the total current escaping the metastable well^{24,25},

$$w \propto \frac{1}{Z} \sum_{k,E} w(k,E) e^{-\beta E + Q_k}. \quad (12)$$

Eq. (12) is a thermal average, weighted with the usual Boltzmann factor $e^{-\beta E + Q_k}$ including the entropy Q_k , of $w(k,E) \sim e^{-S_{WKB}(k,E)}$, the incoherent tunneling amplitude through the barrier of a state with a given energy E and total spin parameter k . The so called reduced action $S_{WKB}(k,E)$ can be obtained by matching the quasiclassical wave functions across the barrier region or following the analytical continuation procedure²¹,

$$\begin{aligned} S_{WKB}(k,E) &= -2 \int_{q_L}^{q_R} dq p(q) \\ &= -N \int_{q_L}^{q_R} dq \operatorname{arccosh} \frac{2(s f(q) - E)}{(1-s) \sqrt{(1-2k)^2 - q^2}}. \end{aligned}$$

The sum Eq. (12) can be approximated by its largest term, the rest being exponentially smaller,

$$w \sim \frac{1}{Z} \sum_{k,E} w(k,E) e^{-\beta E + Q_k} \approx e^{-S_{opt}}. \quad (13)$$

Where the largest term is found by minimizing the action,

$$S_{opt} = S_{WKB} + \beta E - Q_k + \ln Z \quad (14)$$

with respect to k and E ,

$$T(E) \equiv -\frac{\partial S_{WKB}}{\partial E} = \beta \quad (15)$$

$$-\frac{\partial S_{WKB}}{\partial k} - \beta \frac{\partial E}{\partial k} = -\frac{\partial Q_k}{\partial k} \approx \ln \frac{k}{1-k}. \quad (16)$$

where in Eq. (15) fixed k is assumed. Since Q_k is independent of the energy level E the conditions on the optimal tunneling parameters separate into the standard condition Eq. (15) requiring the period of motion in the inverted potential $T(E)$ to match the inverse temperature β ²⁵, and the condition Eq. (16) due to the entropy of states dependent on k , which introduces novel physics in the dynamics of this model. Eqs. (14, 15, 16) need to be supplemented with conditions ensuring that the energy and total spin k are conserved in the tunneling event (we emphasize that we neglect here the effect of the thermal bath during the tunneling event). The tunneling from the metastable well has to be at an energy and spin values, E and k , at which a state exists in the ground state well, i.e. $E \geq \min \{E_R(k)\}$, which is not always satisfied in the system with large entropy of states, i.e. $\mathcal{F}_L < \mathcal{F}_R$ does not necessarily imply $E_L < E_R$.

Eq. (15) has a solution in a range of energies E such that $T_{min} \leq T(E) < \infty$, see inset in Fig. 2 left. In the case of $\beta > T_{min}$ the quantum tunneling process dominates in the sum in Eq. (13). For $\beta < T_{min}$ there are no solutions to Eq. (15) and therefore the optimal energy is at the edge of the interval $E = U(q_{max}) - U(q_{min})$ corresponding to the height of the barrier. In other words, in this regime over-the-barrier escape process dominates with $\beta \sim T_{min}$ being the point of a quantum-to-classical phase transition. Note that the global minimum E_{min} of the function $T(E)$ in the inset in Fig. 2 does not always correspond to the top of the barrier, which means that the quantum to classical transition (in the limit $N \rightarrow \infty$) has a discontinuous 1st order character¹³. Considering Eq. (16) we look for a solution in the interval $0 \leq k \leq k_*$ where k_* is the inflection point of the potential $U(q,k)$ where the right (the ground state) potential well disappears, see Fig. 1, since quantum tunneling conserves the total spin k , for it to occur there must exist states with matching k in the ground state potential well.

The result of this optimization procedure is the optimal action $S_{opt}(\beta)$ at a fixed s shown in Fig. 2. In the vanishing temperature limit $\beta \rightarrow \infty$, where the effect of entropy on the occupation of levels is negligible, $S_{opt}(\beta)$ corresponds to the quantum tunneling from the lowest energy level in the metastable well corresponding to $k = 0$ (horizontal dashed line in Fig. 2 left). As temperature increases (β decreases) the entropy starts playing a role in dynamics and $S_{opt}(\beta)$ increases up to some maximum value, see blue solid line in Fig. 2 left, in contrast with the usual (non-degenerate) case²⁵ where quantum tunneling rate increases with increasing temperature β^{-1} . This is a result of the entropy providing a high statistical weight to the state with suboptimal tunneling rate. This behavior is not entirely generic and originates in the model of Eqs. (1) and (4) because the transverse field lifts the degeneracy of the metastable state favoring the non-degenerate state with $k = 0$, see Fig. 1. Whereas the entropy favors the state with $k = 1/2$ (at $\beta \rightarrow 0$) and therefore with increasing temperature the state with the highest statistical weight will correspond to a finite

$1/2 \geq k > 0$, given by the solution of Eq. (11). At the same time the potential barrier increases with k and therefore the quantum tunneling becomes less and less efficient, resulting in increasing $S_{opt}(\beta)$ with decreasing β up to the regime of the transition into the classical escape at high temperatures $\beta \ll T_{min}$. The classical over-the-barrier excitation is described by the thermal excitation rate $w_{cl} \sim Z^{-1} \exp(-\beta E + Q_k)$. Note that the classical process is driven by the Glauber dynamics of the spins due to the effect of the thermal bath. This process does not conserve the total spin k and therefore the optimal classical trajectory is determined by the saddle point of the free energy (including the entropy) in the 2D space of (k, q) . Entropy provides an additional cost reducing the transition rate which is reflected in the finite offset of the dependence of the classical transition rate on β as $\beta \rightarrow 0$, see black solid line in Fig. 2 Left, see Appendix A for more details. Blue and red dashed lines in Fig. 2 indicate the linear in β dependence of the energy cost of the over the barrier excitation at $k = 0$ and along the line of $q = 1 - 2k$ with the potential maximum at $k \approx k_*$ (the latter is the inflection point of the potential $U(k, q)$), respectively, which correspond to the low temperature potential energy dominated regime and the high temperature entropy dominated regime²⁶.

The steepest descent approximation Eq. (13) is applicable as long as the preexponential factors in the sum are non-divergent which is true away from $\beta \sim T_{min}$ a phase transition point from the quantum tunneling regime to the classical over-the-barrier escape regime²⁵. On general grounds we expect the action to be continuous even in the case where this quantum-to-classical transition is of the 1st order, with the discontinuity occurring in the derivative of the action¹³. Therefore we expect Fig. 2 to provide a qualitatively correct dependence of $S(\beta)$ in the whole range of inverse temperatures β .

III. QUANTUM ANNEALING COMPUTATION TIME

In the course of the QA algorithm the transverse field parameter s is varied from $s = 0$ to $s = 1$ with a fixed rate v at a fixed inverse temperature β . The goal is to find the ground state with probability approaching ~ 1 , allowing for repeated runs of the algorithm. Here we assume that finding any state within the ground state potential well is sufficient to find the solution (as local search could allow identifying the lowest energy state within the well). Given the probability \mathcal{P}_{GS} of finding the ground state after a single run of duration v^{-1} , the number of runs needed to achieve this goal is \mathcal{P}_{GS}^{-1} . The total computation time is therefore given by,

$$\tau \sim v^{-1} \times \mathcal{P}_{GS}^{-1}.$$

The quantum mechanical tunneling rate vanishes as $s \rightarrow 1$ (at very low temperatures of interest here the over-

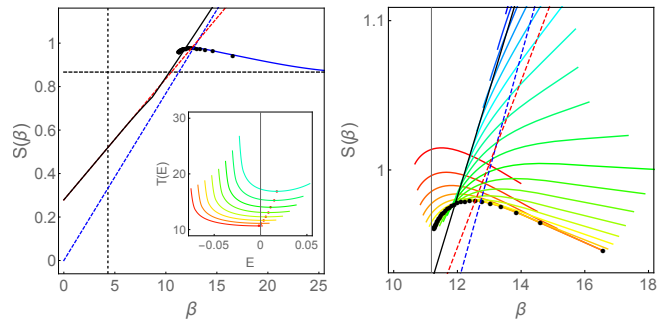


Figure 2. Tunneling action as a function of inverse temperature β . For $q_{min} = 0$, $q_{max} = 0.533$ at $s = 0.85 > s_{QPT}$. *Left*: Black dots, and the solid blue line fit, correspond to optimal finite temperature quantum tunneling action. Horizontal dotted line is the $\beta \rightarrow \infty$ limit of the incoherent tunneling action corresponding to the quantum mechanical tunneling from the lowest level of the metastable well corresponding to $k = 0$. Solid black line corresponds to the optimal action of the classical Glauber dynamics. Blue and red dashed lines show the classical over-the-barrier escape action at $k = 0$ and along the line $q = 1 - 2k$ with the potential maximum at $k_* \approx 0.152$, respectively. The latter, k_* , is the point of inflection, i.e. the point where the minimum of the right potential well merges with the maximum at the barrier top, see Fig. 1. Vertical dashed line corresponds to the temperature driven phase transition point $\beta_{PT} \approx 4.32$ corresponding to equal occupation of the two potential wells. *Inset*: $T(E) = -\partial S/\partial E$ at fixed k which corresponds to the period of quantum mechanical tunneling trajectory in the imaginary time representation. Dominant contribution comes from tunneling at the energy determined from $T(E) = \beta$ for $\beta > T_{min}$, at $\beta < T_{min}$ the transition rate is dominated by the over-the-barrier escape. Different lines bottom to top correspond to different values of s at fixed $k = 0$. Red dots correspond to T_{min} . Note that the minimum $E_{min} : T(E_{min}) = T_{min}$ does not correspond to the highest tunneling energy. This means that the transition from quantum tunneling regime to over-the-barrier escape has discontinuous 1st order character. *Right*: Quantum-classical transition region on a larger scale. Black dots correspond to tunneling action. Different lines show quantum mechanical tunneling action for fixed k , colors correspond to growing $0 \leq k \leq 0.152$ (red to blue). Quantum tunneling process conserves energy and total spin value k . At $k > k_{LR}$ the point where $E_L(k_{LR}) = E_R(k_{LR})$ quantum mechanical tunneling process requires the state in the metastable well to be at an energy $E \geq E_R(k)$ which comes with an additional thermal excitation cost $\beta(E_R(k) - E_L(k))$ in the tunneling action. Therefore for growing k the tunneling action $S(\beta)$ resembles linear classical dependence. Solid black and dashed red and blue lines are the same as in the left figure.

the-barrier transition rate is also weak). Therefore there exists a point $s = s_F$ in the course of the sweep of the transverse field where the relaxation time $\sim w^{-1}(s_F)$ required to achieve thermal distribution becomes longer than the length of the algorithm, $w^{-1}(s_F) \sim v^{-1}$. In other words the computation will be finished before the thermal equilibrium is reached. The system effectively freezes the values of the occupation numbers of the left

\mathcal{P}_L and right \mathcal{P}_R wells at the last point (in the course of the algorithm) where the inter-well transition process was still fast enough (the intra-well relaxation may still be efficient at $s > s_F$). We call this the freezing point. The computation time of the algorithm (its exponential scaling) is therefore determined by the occupation probability $\mathcal{P}_{GS} = \mathcal{P}_R(s_F)$, and the equilibration time $w^{-1}(s_F)$ at the freezing point,

$$\xi \equiv \frac{1}{N} \log \tau \approx \frac{1}{N} \log \left[e^{N S_{opt}} \left(1 + e^{N(\mathcal{F}_R - \mathcal{F}_L)} \right) \right], \quad (17)$$

where S_{opt} is given by Eq. (14), with $s = s_F$. The optimal computation time of the quantum annealing is found by minimizing with respect to the location of s_F and the temperature β at which the computation is performed. The point of the phase transition, $\beta = \beta_{PT}$ and $s_F = s_{PT}$, respectively, defined by, $\mathcal{F}_R - \mathcal{F}_L = 0$ separates two scaling regimes of the computation time,

$$\xi \approx \begin{cases} S_{opt} + \mathcal{F}_R - \mathcal{F}_L, & \beta < \beta_{PT}(s) \\ S_{opt}, & \beta > \beta_{PT}(s) \end{cases} \quad (18)$$

The high temperature limit of this expression is given by the entropy difference between the two wells. This is the limit of local exhaustive search. This is always a bound on the computation time of the algorithm with which we need to compare for completeness. We first consider $\beta < \beta_{PT}$ assuming the free energy of the system demonstrates two minima \mathcal{F}_R and \mathcal{F}_L . In the quantum tunneling regime both $S_{opt}(\beta)$ and $\mathcal{F}_R - \mathcal{F}_L$ decrease with growing β and therefore $\xi(\beta)$ is monotonously decreasing as well. In the classical regime $S_{opt} + \mathcal{F}_R - \mathcal{F}_L$ is also a monotonous function which depending on competition between $S_{opt}(\beta)$ and $\mathcal{F}_R - \mathcal{F}_L$ can be either increasing, in which case $\beta \rightarrow 0$ is the optimal classical computation regime (i.e. the local exhaustive search limit), or decreasing towards the critical point $\beta = \beta_{PT}$. Therefore we need to analyze the performance in the regime $\beta > \beta_{PT}$ and $s > s_{PT}$ and compare it to local exhaustive search. The optimal computation time in this regime, see Eq. (18), is determined by the minimum of the transition rate S_{opt} with respect to β and s .

Because of the concave dependence of $S_{opt}(\beta)$ on the inverse temperature, as shown in Fig. 2 left, the minimum of the action with respect to β corresponds to one of the edges of the inverse temperature interval, i.e. either $\beta = \beta_{PT}$ or $\beta \rightarrow \infty$. The global minimum is therefore the smallest of $S(\beta_{PT}(s_F), s_F)$ and $S(\infty, s_F)$. The minimum with respect to s_F (and therefore the global minimum) is determined by comparing these two functions.

A typical critical line is shown in the left panel of Fig. 3. The inverse critical temperature $\beta_{PT}(s)$, blue solid line in Fig. 3 left, diverges at the point of the quantum phase transition in the course of the algorithm, $s = s_{QPT}$ (vertical dashed line in Fig. 3), and at $s > s_{QPT}$ monotonously decreases with s approaching the classical transition temperature at $s = 1$ (horizontal dashed line in Fig. 3). The

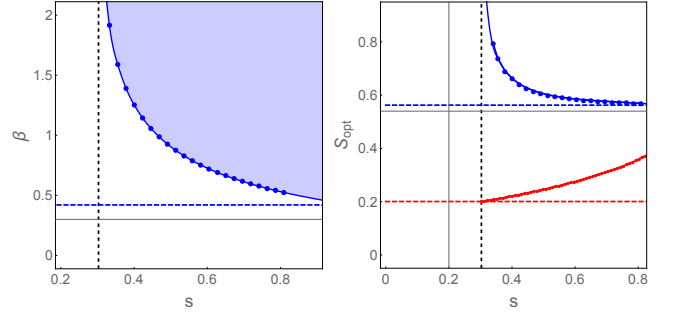


Figure 3. *Left:* Inverse critical temperature dependence on transverse field strength $\beta_{PT}(s)$ for $q_{min} = 0.88$, $q_{max} = 0.955$. The horizontal dashed line corresponds to the classical transition temperature and the vertical dashed line marks the point of the quantum phase transition. *Right:* Blue line shows optimal over-the-barrier escape action along the critical line shown in the left panel. Blue points correspond to the same values of s as in the left figure. Horizontal blue line corresponds to the transition rate at the critical temperature in the classical model, $s = 1$. Vertical line corresponds to the point of zero temperature quantum phase transition. Red line corresponds to the vanishing temperature limit of the quantum tunneling action. Red horizontal dashed line corresponds to the minimum of the quantum tunneling action at the quantum phase transition point. The local exhaustive search corresponds to $\xi = \frac{1}{N} \log \tau_{es} = Q_{cl}(q_{min}) \approx 0.227$, larger than the quantum annealing time.

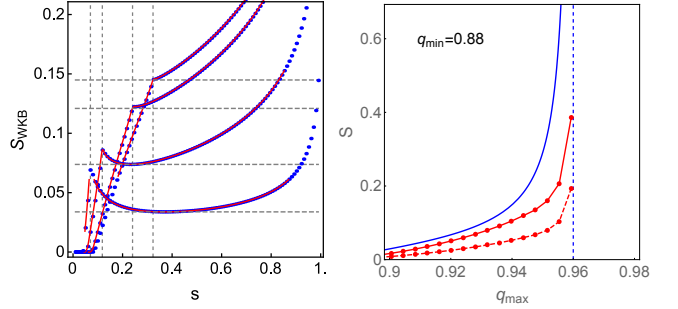


Figure 4. *Left:* Quantum mechanical tunneling action at vanishing temperature in the incoherent regime as a function of the transverse field parameter s . Different curves correspond to different values of $q_{max} = 0.929, 0.946, 0.958, 0.961$ with fixed $q_{min} = 0.9$. Note that the optimal tunneling rate emphasized by horizontal dashed lines does not always correspond to the phase transition point denoted by vertical dashed lines. In other words the optimal QA schedule in the presence of dissipation is crucially different from QA in an isolated system. *Right:* Optimal action for SA (blue) and QA (red) at $q_{min} = 0.88$ for different values of q_{max} . The vertical dashed lines correspond to $q_{min} = \frac{3}{2} q_{max}$ at which point the classical potential has a degenerate ground state at $q = q_{min}$ and $q = 1$. At this point both SA action and QA action diverge, however QA action diverges logarithmically slow in contrast to SA action. For the parameters chosen the local exhaustive search corresponds to $\xi = \frac{1}{N} \log \tau_{es} = Q_{cl}(q_{min}) \approx 0.227$.

right panel of Fig. 3 shows the optimal over-the-barrier escape action at the given critical temperature $\beta_{PT}(s)$, blue (upper) solid line. The blue dots in the left and right panels correspond to the same values of s . The classical action, following the behavior of the inverse critical temperature diverges at the point of the quantum phase transition $s = s_{QPT}$ and decreases with s in the course of the algorithm approaching the value corresponding to the classical model $s = 1$, shown as the blue (upper) dashed line. The latter is the optimum (due to the highest critical temperature) and therefore defines the optimal computation time of the classical simulated annealing algorithm, see Appendix for a more details. The optimum of the quantum action, at vanishing temperature, $\beta \rightarrow \infty$, is given by the tunneling from the bottom of the metastable well. In this limit the entropy does not affect the occupation of the energy levels in the course of the algorithm. We assume that the temperature is still high enough such that there is sufficiently fast intra-well relaxation. Fig. 3 right shows $S_{opt}(\infty, s)$, red (lower) solid line, which assumes the minimal value at the quantum phase transition point $s = s_{QPT}$. Note that this is not true for all the parameter values, instead the minimum of $S_{opt}(\infty, s)$ often occurs at some $s > s_{QPT}$ and its value at this point can be as much as two times smaller than the value at $s = s_{QPT}$, see Fig. 4 left. It is possible to take advantage of this global minimum only in the course of the open system Quantum Annealing since the transition corresponding to this rate maximum occurs not into the ground state level but into one of the excited states. Therefore such a transition should necessarily be followed by relaxation within the local domain of attraction. Such local relaxation is not available in the closed system adiabatic quantum annealing algorithm.

Fig. 3 right demonstrates that the quantum tunneling process may be more efficient than over-the-barrier escape. Both classical and quantum transition rates, and therefore the corresponding computation times, scale exponentially with the system size, $\tau \propto \exp(\alpha N)$, yet the coefficient in the exponent is smaller in the case of QA as compared to the classical simulated annealing, which corresponds to a polynomial speedup. Note that it is important to compare the computation times in Fig. 3 with that of the local exhaustive in the interval $(q_{min}, 1)$, which is the high temperature limit of SA. The corresponding computation time is given by the entropy $\xi = Q_{cl}(q_{min})$, which for parameters considered in Fig. 3, $Q_{cl}(0.88) \approx 0.227$, is above the QA value. We further compare the optimal performance of the open system quantum annealing $S_{opt}(\infty, s)$ to simulated annealing for a wide range of barrier shapes within the cubic model Eq. (4) by varying the location of the metastable minimum q_{min} and the barrier top q_{max} in Eq. (4), see left panel in Fig. 4 and Fig. 5. QA outperforms SA in a range of the parameter space where the potential barrier separating the metastable and the ground states is small. Note that the origin of the speedup in the case considered here is distinct from the standard intuition of thin

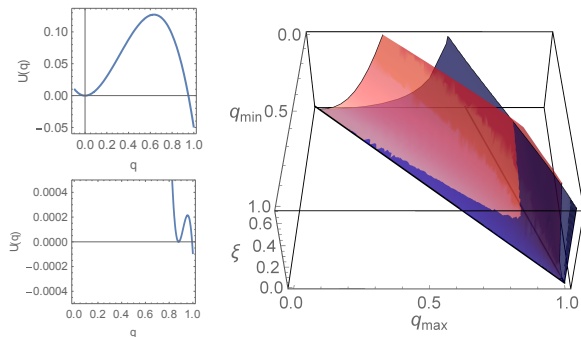


Figure 5. *Left*: Potential barrier between the metastable and the ground state Eq. (4) corresponding to $s = 1$ for two pairs of values (q_{min}, q_{max}) equal to $(0, 0.633)$ (upper plot), $(0.88, 0.955)$ (lower plot). *Right*: Transition action at the optimal freezing point for QA (red) and SA (blue) as a function the location of metastable state q_{min} and the top of the barrier q_{max} . The lower of the two surfaces corresponds to the shorter computation time. QA is advantageous for a range of parameters corresponding to a sufficiently narrow potential barriers. Solid lines in the plane $S = 0$ correspond to $q_{min} = q_{max}$ and $q_{min} = \frac{3}{2}q_{max}$ outlining the range of possible potentials in the cubic model Eq. (4).

and tall barriers favoring quantum tunneling, since the shape of the potential is cubic throughout the range of parameters shown in Fig. 5. Instead the quantum algorithm turns out to be more efficient because it proceeds along a path with lower entropic cost than the path that SA takes. This is a result of the transverse field lifting the degeneracy of the metastable state in the quantum case. Therefore the smallness of the barrier required for the speedup in this case is determined by the comparison of the quantum tunneling action and the SA action including entropy cost of over-the-barrier escape. The latter being a combination of $\beta_{PT}U$ and the additional entropic cost $Q_{cl}(q_{min}) - Q_{cl}(q_{max})$, see Appendix A for details. Note also that the numerical value of the ratio of the logarithms of the normalized computation times $\xi \equiv \frac{1}{N} \log \tau$ for QA and SA can be substantial, see Fig. 4 right.

IV. DISCUSSION

In this paper we considered a model problem for Quantum Annealing that allows analytical investigation and at the same time demonstrates some key features of complex optimization problems, including the discontinuous first order phase transition and the exponential degeneracy of the metastable state. We demonstrate that for problems with extensive degeneracy SA algorithm relies on over-the-barrier escape at very low temperature $\beta \sim O(1)$ as a result the SA computation time is exponential in N . At the same time we show that a computational advantage can be gained using open system quantum annealing

which exploits the effects of thermally assisted tunneling and quantum relaxation. The tunneling occurs between the excited states while the relaxation within the ground state's domain of attraction brings the system down to the lowest energy state at the end of the quantum annealing. Our analysis demonstrates novel and counter intuitive features in the quantum tunneling process caused by the entropy of the metastable states, particularly, the tunneling rate decreasing with increasing temperature. As a consequence we find that the optimal quantum annealing regime corresponds to vanishing temperature, i.e. raising the temperature reduces the efficiency of QA. We also find that at low temperatures the optimal quantum tunneling rate does not always correspond to the point of the phase transition s_{QPT} , in fact tunneling at $s > s_{QPT}$ can have a substantially higher rate, which can be exploited in conjunction with noise-induced thermalization to improve the performance of the algorithm. We find that the comparison of the quantum annealing and simulated annealing comes down to the numerical coefficient in the scaling of the computation time with N , which is determined by the functional form of the potential barrier. We demonstrate that optimal QA could outperform SA in a certain parameter range of our model characterized by small potential barriers. This is in spite of the constrained nature of the quantum tunneling process due to the conservation laws, as opposed to the unconstrained classical Glauber dynamics of SA. We identify an additional advantage the quantum algorithm has over SA, which is the splitting of the degeneracy of the metastable state by the transverse field, which means the quantum algorithm proceeds along a trajectory with lower entropic cost as compared to SA, which is the result of the shape of the effective potential. This suggests a speculation that optimization problems in which en-

tropy is a dominant factor, yet at the same time, which are characterized by a potential energy landscape that can be exploited for more efficient search (as opposed to Grover's unstructured search problem²⁷) may represent a class of problems where quantum annealing could have a computational advantage over simulated annealing.

We also identify key features of the model affecting the performance of the QA, specifically, the quantum fluctuations strength at the phase transition point, and the diverging mass in the quantum kinetic energy which both strongly affect the efficiency of quantum tunneling in the course of the algorithm. We also find that the transverse field term introduces an additional effective potential barrier that has to be overcome in the course of the algorithm. In that respect it would be interesting to use methods developed in this paper to explore QA in mean-field models with different types of driver Hamiltonians whose ground states are not simple product states where ferromagnetic order competes with the transverse (XY) ferromagnetism or superfluidity²⁸⁻³¹.

ACKNOWLEDGMENTS

This work is supported in part by the Office of the Director of National Intelligence (ODNI), Intelligence Advanced Research Projects Activity (IARPA), via IAA 145483; by the AFRL Information Directorate under grant F4HBKC4162G001. The views and conclusions contained herein are those of the authors and should not be interpreted as necessarily representing the official policies or endorsements, either expressed or implied, of ODNI, IARPA, AFRL, or the U.S. Government. The U.S. Government is authorized to reproduce and distribute reprints for Governmental purpose notwithstanding any copyright annotation thereon.

-
- ¹ A. J. Leggett, S. Chakravarty, A. T. Dorsey, M. P. A. Fisher, A. Garg, and W. Zwerger, *Rev. Mod. Phys.* **59**, 1 (1987).
 - ² M. A. Nielsen and I. L. Chuang, *Quantum Computation and Quantum Information: 10th Anniversary Edition*, 10th ed. (Cambridge University Press, New York, NY, USA, 2011).
 - ³ S. Boixo, V. N. Smelyanskiy, A. Shabani, S. V. Isakov, M. Dykman, V. S. Denchev, M. Amin, A. Smirnov, M. Mohseni, and H. Neven, *ArXiv e-prints* (2014), arXiv:1411.4036 [quant-ph].
 - ⁴ J. W. Britton, B. C. Sawyer, A. C. Keith, C.-C. J. Wang, J. K. Freericks, H. Uys, M. J. Biercuk, and J. J. Bollinger, *Nature* **484**, 489.
 - ⁵ T. Kadowaki and H. Nishimori, *Phys. Rev. E* **58**, 5355 (1998).
 - ⁶ S. Geman and D. Geman, *Pattern Analysis and Machine Intelligence*, *IEEE Transactions on PAMI-6*, 721 (1984).
 - ⁷ A. Finnila, M. Gomez, C. Sebenik, C. Stenson, and J. Doll, *Chemical Physics Letters* **219**, 343 (1994).
 - ⁸ J. Brooke, D. Bitko, F. T. Rosenbaum, and G. Aeppli, *Science* **284**, 779 (1999).
 - ⁹ E. Farhi, J. Goldstone, and S. Gutmann, eprint arXiv:quant-ph/0201031 (2002), quant-ph/0201031.
 - ¹⁰ G. E. Santoro, R. Martonak, E. Tosatti, and R. Car, *Science* **295**, 2427 (2002).
 - ¹¹ V. Bapst, L. Foini, F. Krzakala, G. Semerjian, and F. Zamponi, *Physics Reports* **523**, 127 (2013).
 - ¹² P. A. Braun, *Rev. Mod. Phys.* **65**, 115 (1993).
 - ¹³ S. Owerre and M. Paranjape, *Physics Reports* **546**, 1 (2015).
 - ¹⁴ P. Hanggi, P. Talkner, and M. Borkovec, *Rev. Mod. Phys.* **62**, 251 (1990).
 - ¹⁵ Y. Seki and H. Nishimori, *Phys. Rev. E* **85**, 051112 (2012).
 - ¹⁶ B. Seoane and H. Nishimori, *Journal of Physics A: Mathematical and Theoretical* **45**, 435301 (2012).
 - ¹⁷ S. Suzuki, H. Nishimori, and M. Suzuki, *Phys. Rev. E* **75**, 051112 (2007).
 - ¹⁸ S. W. Shin, G. Smith, J. A. Smolin, and U. Vazirani, *ArXiv e-prints* (2014), arXiv:1401.7087 [quant-ph].
 - ¹⁹ T. Jorg, F. Krzakala, J. Kurchan, A. C. Maggs, and J. Pujos, *EPL (Europhysics Letters)* **89**, 40004 (2010).

- ²⁰ V. Bapst and G. Semerjian, *Journal of Statistical Mechanics: Theory and Experiment* **2012**, P06007 (2012).
- ²¹ L. Landau and E. Lifshitz, *Quantum Mechanics: Non-relativistic Theory*, 3rd ed. (Elsevier, 1981).
- ²² P. J. Crowley and A. Green, ArXiv e-prints (2015), arXiv:1503.00651 [cond-mat.mes-hall].
- ²³ B. Zhao, M. C. Kerridge, and D. A. Huse, *Phys. Rev. E* **90**, 022104 (2014).
- ²⁴ D. A. Garanin, X. Martínez Hidalgo, and E. M. Chudnovsky, *Phys. Rev. B* **57**, 13639 (1998).
- ²⁵ E. M. Chudnovsky and J. Tejada, *Macroscopic Quantum Tunneling of the Magnetic Moment* (Cambridge University Press, 2005).
- ²⁶ Note that in the case of the Grover's unstructured search problem a completely flat potential, $U(k, q) = 0$ everywhere except $U(0, 1) = 1$, the offset of the classical action in Fig. 2 corresponds to the classical complexity (computation time) of the Grover's problem with respect to simulated annealing, 2^N . Whereas in presence of the potential profile $U(k, q) \neq 0$ which provides structure to the problem the complexity may be lower.
- ²⁷ L. K. Grover, *Phys. Rev. Lett.* **79**, 325 (1997).
- ²⁸ H. Lipkin, N. Meshkov, and A. Glick, *Nuclear Physics* **62**, 188 (1965).
- ²⁹ N. Meshkov, A. Glick, and H. Lipkin, *Nuclear Physics* **62**, 199 (1965).
- ³⁰ A. Glick, H. Lipkin, and N. Meshkov, *Nuclear Physics* **62**, 211 (1965).
- ³¹ M. P. A. Fisher, P. B. Weichman, G. Grinstein, and D. S. Fisher, *Phys. Rev. B* **40**, 546 (1989).

Appendix A: Simulated Annealing

We discuss the performance of simulated annealing on the model, Eq. (1, 4) in the purely classical case of $s = 1$, see the rightmost panel in Fig. 1. SA algorithm is realized by starting with the infinite temperature limit $\beta \rightarrow 0$, i.e. equal occupation of all states, and reducing the temperature to zero. For simplicity (and without loss of generality) we consider an algorithm where β changes linearly in time from 0 to a very large value with a fixed rate v .

The time it takes to find the ground state with probability approaching ~ 1 , allowing for repeated runs of the algorithm is given, as in the quantum case by,

$$\tau \sim v^{-1} \times \mathcal{P}_{GS}^{-1}.$$

Simulated annealing relies on the system reaching thermal equilibrium throughout at least a part of the algorithm. Such that the ground state occupation is given by the Gibbs distribution. In problems with a free energy barrier separating the initial and the ground state the system's relaxation time is dominated by the over-the-barrier escape probability with $\mathcal{F}(q) = \beta E(q) + Q_{cl}(q)$,

$$w(\beta) \sim \exp(-N(\mathcal{F}(q_{max}) - \mathcal{F}(q_{min}))),$$

given by the statistical weight of the escape trajectory¹⁴ where we include the entropy of the classical state

with magnetization q given by, $Q_{cl}(q) \approx -\frac{1+q}{2} \ln \frac{1+q}{2} - \frac{1-q}{2} \ln \frac{1-q}{2}$. $w(\beta)$ reduces exponentially with decreasing temperature (growing β) and therefore, in analogy with the quantum case considered in the main text, there exists a freezing point $\beta = \beta_F$ in the course of the sweep of the inverse temperature where the relaxation time $\sim w^{-1}(\beta_F)$ required to achieve thermal distribution becomes longer than the length of the algorithm, $w^{-1}(\beta_F) \sim v^{-1}$. After this point the values of the occupation numbers of the left \mathcal{P}_L and right \mathcal{P}_R are effectively frozen. Therefore the computation time is determined by two quantities calculated at the freezing point, the occupation of the ground state potential well $\mathcal{P}_{GS} = \mathcal{P}_R(\beta_F)$, and the relaxation time at the freezing point $w^{-1}(\beta_F)$,

$$\tau \approx e^{N(\mathcal{F}(q_{max}) - \mathcal{F}(q_{min}))} \left(1 + e^{N(\mathcal{F}(1) - \mathcal{F}(q_{min}))}\right), \quad (\text{A1})$$

where we keep only the main order in the limit $N \rightarrow \infty$ such that $\mathcal{P}_{GS}(\beta_F) \approx \exp(-\mathcal{F}(1))/(\exp(-\mathcal{F}(1)) + \exp(-\mathcal{F}(q_{min})))$. The optimal computation time can be obtained by minimizing with respect to the inverse temperature at the freezing point, $\frac{\partial}{\partial \beta_F} \left(\frac{1}{N} \log_2 \tau\right) = 0$. This derivative is discontinuous at the point of the phase transition β_{PT} , where $\mathcal{F}_R - \mathcal{F}_L = 0$. The computation time is an increasing function at $\beta_F > \beta_{PT}$, as it is dominated by the decreasing transition rate, the prefactor in front of the curly brackets in Eq. (A1). Whereas it can be either monotonously decreasing or increasing function at $\beta_F < \beta_{PT}$ depending on the competition between the prefactor and the exponents in the brackets in Eq. (A1). Therefore the global minimum of $\tau(\beta_F)$ corresponds to the smallest value out of $\tau(\beta_{PT})$ and $\tau(0) \approx 2^N$, in the decreasing and increasing case respectively. The latter corresponding to the exhaustive search, i.e. 2^N repetitions of infinitely fast SA. The ground state at $q = 1$ is unique $Q(1) \approx 0$ therefore the point of the classical phase transition is at $\beta_{PT} = \frac{Q(q_{min})}{E(q_{min}) - E(1)}$. Therefore the optimal SA computation time corresponds to the smaller of the two values,

$$\tau \rightarrow \left[\exp \left[N \left(\frac{E(q_{max}) - E(q_{min})}{E(q_{min}) - E(1)} Q(q_{min}) + \delta Q \right) \right] \right], \quad 2^N,$$

where $\delta Q \equiv Q(q_{min}) - Q(q_{max})$. Note that the entropy associated with the metastable state causes a very low transition temperature $\beta_{PT} \sim O(1)$ and gives rise to an additional statistical factor $\exp(\delta Q)$ slowing down the transitions over the barrier. This additional factor appears as a prefactor in the Kramers rate calculation¹⁴, in the model considered here this factor is exponential and needs to be included to correctly describe the scaling of the classical transition rate with N .

Appendix B: Eigenstates overlap

One of the characteristics associated with complexity of a given problem for quantum annealing algorithm is the overlap of the eigenstate wave functions at the beginning and the end of the algorithm. We analyze it for our model Eqs. (1, 4). The initial state $s = 0$ is characterized by the maximal x -projection of the total spin,

$$\hat{S}^x \left| \frac{N}{2} - K \right\rangle_x = \left(\frac{N}{2} - K \right) \left| \frac{N}{2} - K \right\rangle_x .$$

The overlap of this state with the solution of the classical problem - state fully polarized along z -axis is,

$${}_x \langle N/2 - K | \vec{0} \rangle = \left[\frac{1}{2^N} \binom{N}{K} \right]^{1/2} .$$